Kinetic Mechanism and Quaternary Structure of *Aminobacter aminovorans* NADH:Flavin Oxidoreductase: An Unusual Flavin Reductase with Bound Flavin†

Thomas R. Russell,‡ Borries Demeler,§ and Shiao-Chun Tu*,‡,||

Departments of Biology and Biochemistry and of Chemistry, University of Houston, Houston, Texas 77204-5001, and Department of Biochemistry, The University of Texas Health Science Center, San Antonio, Texas 78229-3900

Received September 3, 2003; Revised Manuscript Received December 3, 2003

ABSTRACT: The homodimeric NADH:flavin oxidoreductase from *Aminobacter aminovorans* is an NADH-specific flavin reductase herein designated FRD_{Aa}. FRD_{Aa} was characterized with respect to purification yields, thermal stability, isoelectric point, molar absorption coefficient, and effects of phosphate buffer strength and pH on activity. Evidence from this work favors the classification of FRD_{Aa} as a flavin cofactor-utilizing class I flavin reductase. The isolated native FRD_{Aa} contained about 0.5 bound riboflavin-5′-phosphate (FMN) per enzyme monomer, but one bound flavin cofactor per monomer was obtainable in the presence of excess FMN or riboflavin. In addition, FRD_{Aa} holoenzyme also utilized FMN, riboflavin, or FAD as a substrate. Steady-state kinetic results of substrate titrations, dead-end inhibition by AMP and lumichrome, and product inhibition by NAD^+ indicated an ordered sequential mechanism with NADH as the first binding substrate and reduced FMN as the first leaving product. This is contrary to the ping-pong mechanism shown by other class I flavin reductases. The FMN bound to the native FRD_{Aa} can be fully reduced by NADH and subsequently reoxidized by oxygen. No NADH binding was detected using 90 μM FRD_{Aa} apoenzyme and 300 μM NADH. All results favor the interpretation that the bound FMN was a cofactor rather than a substrate. It is highly unusual that a flavin reductase using a sequential mechanism would require a flavin cofactor to facilitate redox exchange between NADH and a flavin substrate. FRD_{Aa} exhibited a monomer−dimer equilibrium with a K_d of 2.7 μM. Similarities and differences between FRD_{Aa} and certain flavin reductases are discussed.

Reduced flavin is a critical mediator for a variety of metabolic reactions. In isolation or in association with enzymes, such as monofunctional monooxygenases, it is required for processes such as bioluminescence, reduction of ribonucleotides, generation of superoxide radicals, iron release from ferrisiderophores, degradation of aromatic compounds such as 4-hydroxyphenylacetate, biosynthesis of antibiotics (valanimycin, actinorhodin, and pristinamycin), fossil fuel desulfurization, degradation of amino acid derivatives such as pyrrole-2-carboxylate, degradation of synthetic chelating agents (NTA[1] and ethylenediaminetetraacetate), biosynthesis of chorismate, repair of photochemically damaged DNA, and reduction of methemoglobin (*1*). A major class of enzymes responsible for the production of reduced flavin is NAD(P)H:flavin oxidoreductases (flavin reductases).

Flavin reductases catalyze the following reaction:

$$F + NAD(P)H + H^+ \rightarrow FH_2 + NAD(P)^+ \qquad (1)$$

where F is the oxidized flavin substrate and FH_2 is the reduced flavin product. F is most commonly FMN, but many enzymes have the ability to also utilize riboflavin and FAD, and in some cases they are the preferred substrates (*2*, *3*). Due to the growing number and diversity of flavin reductases, a classification system was developed to organize the study of these enzymes (*1*). It has been proposed that NADH- and NADPH-preferring flavin reductases be named FRD and FRP, respectively, while those general flavin reductases that use both pyridine nucleotides with similar efficiency be named FRG. We now propose that a subscript could be added to indicate the source of the enzyme. Since some flavin reductases have a flavin cofactor and some do not, flavoproteins are termed class I whereas nonflavoenzymes are designated class II. These two classes have marked differences in their amino acid sequences and folding motifs. More striking though is the differences in their kinetic mechanisms.

It has been found that class I flavin reductases utilize ping-pong kinetics. FRP I from *Vibrio harveyi* and FRG/FRase I

† Supported by Grants GM25953 from the National Institutes of Health and E-1030 from the Robert A. Welch Foundation. The development of the UltraScan software is supported by the National Science Foundation through Grant DBI-9974819 to B.D.

* To whom correspondence should be addressed. Phone: (713) 743-8359. Fax: (713) 743-8351. E-mail: dtu@uh.edu.

‡ Department of Biology and Biochemistry, University of Houston.

§ The University of Texas Health Science Center.

|| Department of Chemistry, University of Houston.

[1] Abbreviations: NTA, nitrilotriacetate; DEAE-cellulose, diethylaminoethylcellulose; FAD, flavin adenine dinucleotide; FMN and $FMNH_2$, oxidized and reduced riboflavin-5′-phosphate, respectively; FRD, NADH-preferring flavin reductase; FRD_{Aa} and $apoFRD_{Aa}$, the holoenzyme and apoenzyme, respectively, of FRD from *Aminobacter aminovorans*; FRG, NADH- and NADPH-utilizing general flavin reductase; FRP, NADPH-preferring flavin reductase; Gnd·HCl, guanidine hydrochloride; IPTG, isopropyl β-D-thiogalactose; LB, Luria−Bertani; MWCO, molecular weight cut off; NmoA and NtaA, nitrilotriacetate monooxygenase component A; NmoB and NtaB, nitrilotriacetate monooxygenase component B; PCR, polymerase chain reaction; pI, isoelectric point.

10.1021/bi035578a CCC: $27.50
Published on Web 01/21/2004

from *Vibrio fischeri* (both required for bioluminescence in association with the monofunctional monooxygenase bacterial luciferase) have been extensively characterized (*4*−*12*) and serve as models for the FR(P,G) I schemes. The class II enzymes have been found to use sequential kinetics. FRII (Fre) from *Escherichia coli* is the most characterized for this class (*2*, *3*, *13*−*17*). Fre does not fit well into any of the FR(D,P,G) schemes. It is unusual in that it is an FRG with riboflavin as the cosubstrate, but it is an FRD with FMN (*2*) or FAD (*14*); the latter has recently been shown to be the preferred flavin substrate and an inhibitor for this reductase (*3*). Thus, it does not serve as a general model for the FRD enzymes. The FRD enzymes, class I or II, are the "missing link" in the sense that it is the one group of flavin reductases for which only limited understanding of their general characteristics is available.

Since the class I FRP and FRG have already been extensively studied, this work aimed at extending our investigation to a reductase of the class I FRD type. The flavin reductase NmoB (NtaB) from *Chelatobacter heintzii* ATCC 29600 (the preferred binomial nomenclature is now *Aminobacter aminovorans*) contained bound FMN and showed a strong preference for NADH (*18*). Hence, this reductase, herein referred to as FRD_{Aa}, was targeted for investigation. Being a dimer, with a monomer molecular mass of 34.5 kDa (*18*, *19*), it is by far the largest of the flavin reductases that have at least been partially characterized. It is believed to be responsible for the in vivo supply of $FMNH_2$ to NmoA (NtaA), the monofunctional monooxygenase responsible for the initial reaction in the catabolism of NTA (*18*−*21*) via conversion of magnesium-complexed NTA to iminodiacetate and glyoxylate through the following reaction:

$$Mg^{2+}{-}N(CH_2COO^-)_3 + FMNH_2 + O_2 \rightarrow HN(CH_2COO^-)_2 + H(CO)COO^- + FMN + H_2O + Mg^{2+} \quad (2)$$

Since the discovery of FRD_{Aa} over a decade ago, its enzymatic properties remained largely unexplored. This study was conducted not only to determine the basic characteristics of this enzyme, but more importantly to determine the nature of its subunit interaction and kinetic mechanism in comparison with those of other flavin reductases. *V. harveyi* FRP and *V. fischeri* FRG/FRase I both undergo a monomer−dimer equilibrium (*7*, *11*). Moreover, the subunit dissociation of *V. harveyi* FRP has a critical functional consequence; only the monomeric FRP forms a complex with luciferase (*22*). For FRD_{Aa}, we found that this enzyme does not just exist as a dimer (*18*) but assumes a monomer−dimer equilibrium. It was expected at the beginning of this study that FRD_{Aa}, on the assumption that the bound FMN is a cofactor, would display ping-pong kinetics similar to those of FRP I and FRG/FRase I. The unexpected results will make the case that, despite that FRD_{Aa} was found to bind one flavin per monomer as a cofactor, the reductase holoenzyme exhibited a rather unusual ordered sequential mechanism by binding, per monomer, an NADH as the first substrate and an additional flavin molecule as the second substrate. Preliminary results of this work were reported earlier in an abstract (*23*).

EXPERIMENTAL PROCEDURES

Materials. FMN, FAD, riboflavin, NADH, NADPH, NAD^+, and AMP were from Sigma. Lumichrome was from Aldrich. Urea was from EM Science. IPTG, dithiothreitol, Gnd·HCl, restriction enzymes, *Pfu* DNA polymerase, T4 DNA ligase, *E. coli* JM109 competent cells, and the Wizard SV Plus Miniprep kit were from Promega. Vector pUC19 was from NEB. The Qiaex II gel extraction kit was from Qiagen. Oligonucleotide primers were from MWG Biotech. Ultrafiltration membranes were from Millipore. DEAE-cellulose DE-52 was from Whatman. DEAE-Sepharose resin and the HiLoad 16/60 Superdex 200 pg column were from Amersham. All isoelectric focusing supplies, the Bradford and Lowry protein concentration reagents, and bovine serum albumin were from Bio-Rad. Phosphate (P_i) buffers were pH 7.8 (adjusted from 7.0 to 7.8 with 5 M NaOH) and consisted of mole fractions of 0.39 sodium monobase and 0.61 potassium dibase in deionized water.

Cloning. Plasmid pTF2 (expression vector pTrc99A containing *nmoB*) was a generous gift from Dr. Luying Xun (Washington State University) (*20*). The *nmoB* gene (herein named *frd*) was isolated from the host *E. coli* JM105 cells with the Wizard SV Plus Miniprep kit and was subcloned into pUC19 by PCR. The forward primer 5′-TT*GCATGC*-TATGGCAGACCAAATTCGATCGGCAA-3′ contained a restriction site for *Sph*I (italic), and the reverse primer 5′-TTT*CTAGA*AATTAGCTAGACCCGCGCCCCGGGCC-3′ contained a restriction site for *Xba*I (italic). *Pfu* DNA polymerase and the primers were used to extract *frd* from pTF2 using the following PCR protocol: (1) 94 °C for 3 min, (2) 94 °C for 1 min, (3) 54 °C for 2 min, (4) 68 °C for 3 min, (5) repeat 27 times steps 2−4, and (6) repeat steps 2 and 3 once, followed by a final elongation at 68 °C for 8 min (*24*). The linearized PCR product was agarose gel purified using the Qiaex II gel extraction kit. The PCR product and pUC19 were restriction digested with *Sph*I and *Xba*I in a water bath at 37 °C for 2 h followed by a 20 min incubation at 65 °C to heat kill the enzymes (*24*). The PCR product and pUC19 were both agarose gel purified as before and ligated with T4 DNA ligase in a water bath at 16 °C for 1 h (*24*). The ligation reaction was used to transform *E. coli* JM109 competent cells by heat shock according to the protocol included with the kit. Positive transformants were selected by blue/white screening with IPTG and X-gal (5-bromo-4-chloro-3-indolyl-β-D-galactose). The *frd* gene was verified to be in frame with pUC19 (plasmid name $pFRD_{Aa}$) through sequencing performed at Lone Star Labs (Houston, TX).

Purification of FRD_{Aa}. *E. coli* JM109 harboring $pFRD_{Aa}$ was grown overnight on an LB plate containing 100 μg/mL ampicillin (the working concentration for all subsequent growth media) at 37 °C. A single colony was then used to inoculate 50 mL of LB, which was grown for 12 h at 37 °C. Twelve flasks each containing 1 L of 2 × LB were each inoculated with 1 mL of the starter culture, and the cells were grown at 37 °C and 250 rpm until 0.6 OD_{600} was achieved (∼4 h). A final IPTG concentration of 1 mM was added to each culture, and they were allowed to continue

growing for another 20 h under the same, constant conditions. The cultures were centrifuged, to 35 g of wet cell paste was added 300 mL of 50 mM P_i (all buffers used for purification and storage contained 1 mM dithiothreitol), and the resuspended cells were sonicated on ice for 20 min. The cell debris was removed from the crude lysate by centrifugation at 10000*g* for 25 min. To the crude lysate was added 50 g of DEAE-cellulose DE-52, and the suspension was stirred on ice (all subsequent steps were performed at room temperature, ~23 °C) for 1 h. The resin was washed with 50 mM P_i until the eluate was clear (~400 mL). FRD_{Aa} was recovered by elution with 300 mM P_i. The fraction was diluted 6-fold with deionized water and loaded onto a 2.5 × 15 cm DEAE-Sepharose column equilibrated with 50 mM P_i. The sample was washed with 5 column volumes of 50 mM P_i, followed by isocratical elution with 160 mM P_i. Active fractions were pooled and concentrated to 2 mL by ultrafiltration using a 30000 MWCO poly(ether sulfone) membrane. The sample was loaded onto a Superdex 200 gel filtration column, equilibrated with 160 mM P_i. The eluted FRD_{Aa}-containing fractions were combined and then dialyzed to give a final P_i concentration of 50 mM. They were stored as aliquots at −20 °C. FRD_{Aa} was determined to be 90% pure on the basis of analysis of an SDS−PAGE (*24*) gel image with SigmaGel gel scanning software.

Preparation of the Apoenzyme and Reconstitution of the Holoenzyme. The apoenzyme was prepared with a Gnd·HCl/urea denaturation column, and renatured by dilution into swirling P_i buffer using previously published methods (*7*, *11*). Reconstitution of the holoenzyme was performed by mixing the renatured apoenzyme with excess FMN. Free FMN was removed from the reconstituted holoenzyme by molecular sieve chromatography.

Optical Spectroscopy. Absorption spectra or absorbance measurements at a desired wavelength were obtained by using a Varian Cary 50 Bio UV−vis spectrophotometer. The molar absorption coefficient (ϵ_{280}) was determined spectrophotometrically with 6 M Gnd·HCl in 50 mM P_i using the method of Gill and von Hippel (*25*). Circular dichroism spectra were measured using 10 μM enzyme in an OLIS DSM 1000 CD spectrophotometer.

Isoelectric Focusing. The pI was determined using a pH 3−10 gradient isoelectric focusing gel. The anode buffer was 7 mM phosphoric acid, and the cathode buffer was 20 mM lysine/20 mM arginine. The gel was electrophoresed with the following protocol: (a) 100 V for 1 h, (b) 250 V for 1 h, and (c) 300 V for 45 min. It was stained with a Coomassie Blue/Crocein Scarlet solution.

Flavin and NADH Binding. The FMN:dimeric FRD_{Aa} ratio following purification of the native FRD_{Aa} was determined by comparing the concentration of bound FMN (determined spectrophotometrically at 455 nm using a molar absorption coefficient of 1.25×10^4 M^{-1} cm^{-1}) to protein. The FMN:dimeric FRD_{Aa} ratio was also determined following saturation with FMN using equilibrium ultrafiltration (*26*) with a 30000 MWCO poly(ether sulfone) membrane. The binding of riboflavin to the native FRD_{Aa} and that of NADH by the apoFRD_{Aa} were similarly determined. The stoichiometry and K_d of FMN binding to the apoenzyme of FRD_{Aa} were also determined by fluorescence quenching of the enzyme upon FMN titration. Excitation was set at 295 nm, and emission was monitored at 330 nm using a Varian Cary Eclipse fluorescence spectrophotometer. Inner filter effects on excitation and emission due to high concentrations of FMN were corrected using the relationship (*27*)

$$F_{\text{corrected}} = F_{\text{observed}} \times 10^{-0.5 \times l_{ex} \times A_{ex}} \times 10^{-0.5 \times l_{em} \times A_{em}} \quad (3)$$

where l_{ex} and l_{em} are, respectively, the cuvette full path length (cm) along the direction of excitation and emission light and A_{ex} and A_{em} are, respectively, absorbance of the sample (at a 1 cm light path) at the excitation and emission wavelength settings.

Spectrophotometer Assays. Flavin reductase activities were measured at 23 °C by monitoring the A_{340} decrease associated with the oxidation of NADH in a 1 cm light path. All reactions were initiated by adding NADH into 1 mL of 50 mM P_i containing 1 μM FRD_{Aa} (calculated using a monomer molecular mass of 34.5 kDa) and a designated concentration of the flavin species specified. Unless otherwise stated, FRD_{Aa} in the isolated native form (containing ~0.5 FMN per enzyme monomer) was used for activity measurements. For standard assays, substrates were added at 2.5 μM for FMN and 320 μM for NADH. The concentrations of NADH were determined from A_{340} measurements using $\epsilon_{340} = 6.22 \times 10^3$ M^{-1} cm^{-1}. When assays were performed at temperatures other than 23 °C (the temperature stability profile assays), all solutions were incubated at the stated temperature for 30 min prior to assay under standard conditions. Lumichrome was dissolved in a 50 mM NaOH stock solution. It was stable for the duration of the assay, and had no affect on the assay buffer pH. The pH profile was determined by measuring the activity of FRD_{Aa} in 50 mM P_i at various pH values.

Anaerobic Reduction of FRD_{Aa} by NADH. A 200 μL sample of NADH and 800 μL of FRD_{Aa} were aliquoted into the side arm and built-in cuvette, respectively, of a sealed glass tonometer. Repeated evacuations and equilibrations with ultra-high-purity-grade nitrogen gas were performed over a 4 h time period to generate the anaerobic atmosphere. Mixing and reduction were initiated by tilting the tonometer to allow the NADH solution to pour into the built-in cuvette containing FRD_{Aa}.

Analytical Ultracentrifugation. All sedimentation equilibrium experiments were performed with a Beckman Optima XL-I at the Center for Analytical Ultracentrifugation of Macromolecular Assemblies (CAUMA; Department of Biochemistry, The University of Texas Health Science Center at San Antonio). Equilibrium and Monte Carlo analyses were performed with UltraScan version 6.1 (http://www.ultrascan.uthscsa.edu). Hydrodynamic corrections for buffer conditions were made according to data published by Laue et al. (*28*) and as implemented in UltraScan. The partial specific volumes of the peptides were estimated according to the method of Durchschlag (*29*) and as implemented in UltraScan. Data were fitted to multiple models. The most appropriate model was chosen on the basis of visual inspection of the residual run patterns and on the basis of the best statistics. Confidence intervals of 95% were determined by Monte Carlo analysis. Monte Carlo analyses were calculated on a 40-processor Linux Beowulf cluster running Slackware Linux version 9.0. All samples were analyzed in a buffer containing 160 mM phosphate, pH 7.8. Sedimentation equilibrium experiments were performed at 4 °C and

speeds ranging between 15000 and 38000 rpm. Absorbance samples were spun in six-channel Epon/charcoal centerpieces in the AN-50-TI rotor, and Rayleigh interference samples were spun in two-channel Epon/charcoal centerpieces. Scans were collected at equilibrium at 230 and 280 nm, and using interference optics in radial step mode with a 0.001 cm step size setting and 20-point averages. Multiple loading concentrations ranging between 0.3 and 0.7 A were measured at the given wavelength, and data exceeding 0.9 A were excluded from the fit. Interference samples were loaded with concentrations of 1, 1.5, and 2 mg/mL. Data in the concentration range of 0−35 μM were examined. Wavelength scans were performed between 220 and 340 nm for each concentration and globally fitted to a global molar absorption profile using UltraScan. The molar absorption profile was normalized with the molar absorption coefficient at 280 nm by estimation from the protein sequence according to the method of Gill and von Hippel (*25*) and as implemented in UltraScan.

Protein Concentration. Since the molar absorption coefficient was not available at the beginning of this study, the concentration of FRD_{Aa} for most assays was determined by the method of Bradford (*30*) with bovine serum albumin as a standard. The Lowry assay (*31*) with bovine serum albumin as a standard was used for determining the final FRD_{Aa} concentration for the FMN stoichiometry analysis.

RESULTS

General Characterization of FRD_{Aa}. The yields of FRD_{Aa} purification were variable, ranging from 10 to 120 mg of purified enzyme from 35 g of wet cell paste, but on average the yield was approximately 35 mg. The experimentally determined values of the molar absorption coefficient and pI were 2.5×10^4 M^{-1} cm^{-1} at 280 nm and 5.1, respectively. The latter is similar to the pI 5.5 predicted earlier (*19*). The experimental molar absorption coefficient was found to give FRD_{Aa} concentrations within ±5% of that determined by the Bradford assay.

The thermal stability of FRD_{Aa} was determined by incubating the enzyme at various temperatures for 30 min. This reductase was stable between 0 and 30 °C. About 56% and 3% activity remained at 40 and 50 °C, respectively. The highest activity levels of FRD_{Aa} were found in 50−100 mM P_i, with 15% activity remaining in deionized water, and 56% activity remaining with 850 mM P_i. The pH profile of FRD_{Aa} is a bimodal curve with a primary maximum at pH 8.5 and a secondary maximum at pH 5.2 (Figure 1).

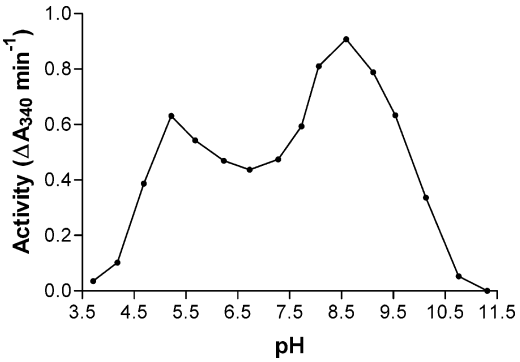

FIGURE 1: pH−activity profile of FRD. All samples (●) were assayed in 50 mM P_i at the stated pH. Substrates were at 2.5 μM for FMN and 320 μM for NADH. No activity was detected beyond pH 3.5 or 11.5. FRD had 70% of the activity at the secondary pH optimum of 5.2 compared to the primary pH optimum of 8.5.

Flavin and NADH Binding. Following purification, a 10 μM aliquot of FRD_{Aa} was determined to have a bound FMN concentration of 4.9 μM. This gives an approximate ratio of one FMN per FRD_{Aa} dimer. Next, the isolated FRD_{Aa} was examined for possible additional binding of FMN. To 10 μM FRD_{Aa} was added 41.5 μM FMN, and the mixture was incubated for 15 min. The sample volume was halved in the ultrafiltration cell, and the concentrations of FRD_{Aa} and FMN were determined for both the retentate and filtrate. The concentration of FRD_{Aa} in the retentate increased from 10 to 20 μM. The total concentration of FMN in the enzyme sample before filtration was 46.4 μM (41.5 μM free FMN + 4.9 μM bound FMN), which increased to 52.6 μM FMN in the retentate following filtration. Free FMN in the filtrate was 34 μM after filtration. Thus, the final concentration of FRD_{Aa}-bound FMN was 18.6 μM. Since the final concentration of FRD_{Aa} was 20 μM and it was approximately 90% pure, this indicates the binding of one FMN per FRD_{Aa} monomer. The final FRD_{Aa} concentration was also determined with the Lowry assay, and was found to be 18.6 μM. This gives a ratio of exactly one FMN per FRD_{Aa} monomer.

The binding of riboflavin by FRD_{Aa} was similarly determined. When a native FRD_{Aa} sample (10 μM of FRD_{Aa} with 3.3 μM bound FMN) was mixed with 38.3 μM riboflavin and subjected to ultrafiltration, the enzyme retained 0.52 bound flavin per monomeric FRD_{Aa}. Since FMN and riboflavin were quantified by absorbance at 455 nm and both flavins have the same molar absorption coefficient, exactly how much of the bound flavin was riboflavin was not determined. Nonetheless, our results indicated a minimal binding of 0.19 riboflavin per FRD_{Aa} monomer. When the same experiment was repeated but with riboflavin exogenously added at 127 μM, the enzyme retained one bound flavin per FRD_{Aa} monomer after ultrafiltration. This indicated a minimal binding of 0.67 riboflavin per FRD_{Aa} monomer, but the binding affinity of riboflavin was considerably weaker than that of FMN.

Apoenzyme was obtained from the native FRD_{Aa} following a denaturation−renaturation procedure (*7*, *11*). Usually a few percent of the bound FMN was still retained in the apoenzyme so obtained. Using an apoenzyme sample containing 8% FMN, the stoichiometry and K_d for FMN binding were determined by monitoring FRD_{Aa} fluorescence quenching. First, 5 μM apoFRD_{Aa} was titrated with various amounts of FMN. Higher levels of protein fluorescence quenching were observed at increasing concentrations of FMN when the [FMN]/[monomeric apoenzyme] molar ratios were <1.0. In contrast, very few changes in protein fluorescence were detected when [FMN]/[monomeric apoenzyme] molar ratios were >1.0. The extrapolated break point of such a fluorescence quenching curve corresponded to a binding of 0.8 FMN per apoFRD_{Aa} monomer (Figure 2A). Together with the 8% bound FMN retained in the starting apoFRD_{Aa} sample, this reductase was found to bind 0.9 FMN per monomer, correlating well with the 1:1 binding of FMN by FRD_{Aa} monomer shown by ultrafiltration as mentioned above. A limiting amount (0.2 μM) of apoFRD_{Aa} was also titrated with increasing levels of FMN, and changes in FRD_{Aa} fluorescence (Δ(fluorescence) defined as the fluorescence of apoFRD_{Aa} without any addition of FMN minus that after

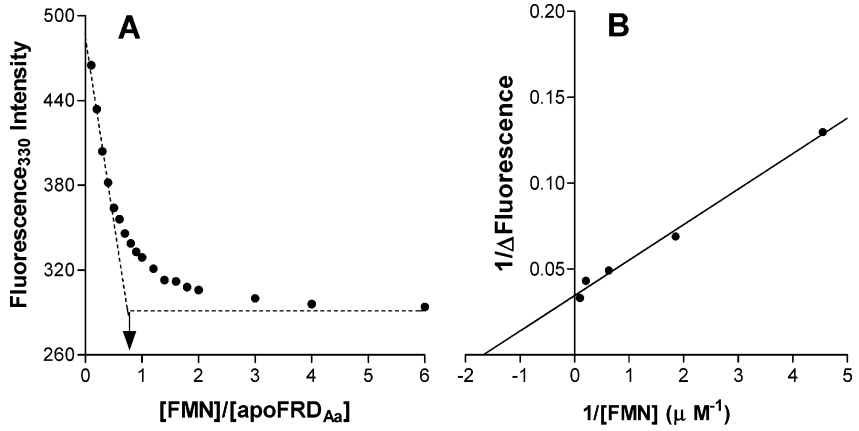

FIGURE 2: Fluorometric titrations of apoFRD$_{Aa}$ with FMN. (A) A constant amount of apoFRD$_{Aa}$ at 5 μM monomeric concentration was titrated with FMN in 50 mM P_i at various molar ratios as indicated. Emission intensities at 330 nm were measured using an excitation at 295 nm, and are plotted against the molar ratio of [FMN]/[apoFRD$_{Aa}$]. For samples containing $\geq$3 μM FMN, observed ApoFRD$_{Aa}$ fluorescence intensities were corrected for the inner filter effects of FMN on both excitation and emission as described in the Experimental Procedures. (B) ApoFRD$_{Aa}$ at 200 nM was titrated with several levels of FMN as indicated. Following incubation for 5 min at each concentration, fluorescence intensities at 330 nm were measured using an excitation at 300 nm. Δ(Fluorescence) is defined as the emission intensity of apoFRD$_{Aa}$ minus that with the designated concentration of FMN. Data are shown as a double reciprocal plot.

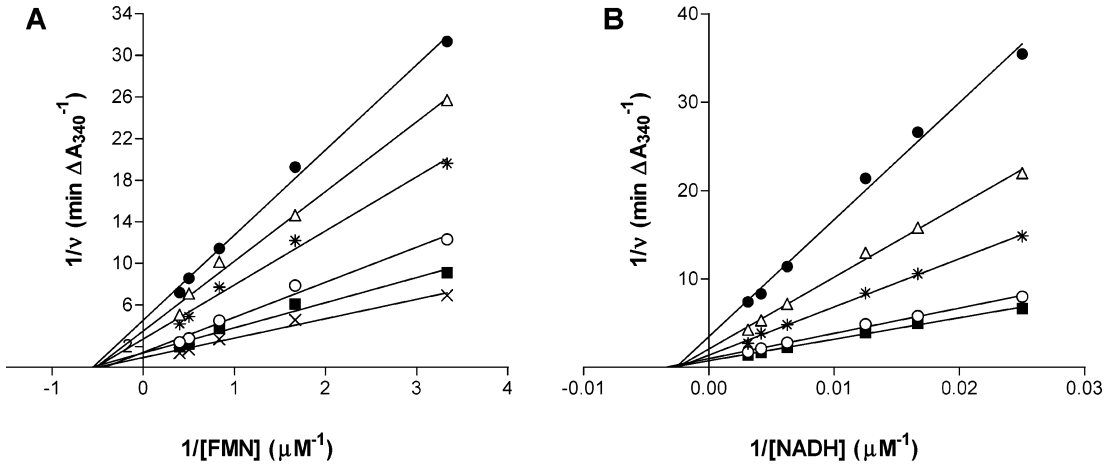

FIGURE 3: Steady-state kinetics of FRD$_{Aa}$ as a function of substrate concentration: double reciprocal plots of the initial velocity (v) of FRD$_{Aa}$ (A) as a function of FMN concentration in the presence of 40 (●), 60 (△), 80 (∗), 160 (○), 240 (■), and 320 (×) μM NADH and (B) as a function of NADH concentration in the presence of 0.3 (●), 0.6 (△), 1.2 (∗), 2.0 (○), and 2.5 (■) μM FMN.

the addition of a designated level of FMN) were determined. A double reciprocal plot of the Δ(fluorescence) versus concentration of added FMN gives a linear line (Figure 2B), and a K_d of 0.6 μM was obtained from the abscissa intercept. Finally, using the ultrafiltration technique, no NADH binding was detected at 90 μM apoFRD$_{Aa}$ and 300 μM NADH.

Steady-State Kinetics. For bisubstrate−biproduct (Bi Bi) reactions, Lineweaver−Burk plots of initial velocities versus substrate concentrations give a set of parallel lines for the ping-pong mechanism and a set of lines intersecting to the left of the ordinate for the sequential mechanism (*32*, *33*). Flavin reductase activity was determined as a function of FMN concentration at several levels of NADH (Figure 3A) and as a function of NADH concentration at several levels of FMN (Figure 3B). In both cases, a series of intersecting lines were obtained, hence indicating a sequential mechanism for FRD$_{Aa}$. On the basis of results shown in Figure 3, secondary plots of $1/v$ from the ordinate intercept versus the reciprocal of its respective concentration of the constant substrate are used to calculate critical kinetic constants. Results gave rise to values of maximal specific activity (V_{max}) of 8.4 $\pm$ 1.3 (μmol/min)/mg, $K_{m,NADH}$ = 0.35 mM, and $K_{m,FMN}$ = 1.3 μM. FRD$_{Aa}$ also utilized riboflavin and FAD as substrates, exhibiting $K_{m,flavin}$ and V_{max} values of 5.8 μM and 10.8 (μmol/min)/mg, respectively, for riboflavin and 1.7 μM and 7.6 (μmol/min)/mg, respectively, for FAD. It is possible that riboflavin and/or FAD could be active as a cofactor. If so, the addition of riboflavin and FAD may lead to the formation of more than one active holoenzyme species, the distribution of which in our assay solutions cannot be qualified without further studies. Hence, the K_m and V_{max} values reported above for riboflavin and FAD should be viewed as apparent values.

Inhibition studies were employed to identify whether FRD$_{Aa}$ follows an ordered or random sequential Bi Bi mechanism (*34*). When the activity of FRD$_{Aa}$ was determined at a fixed FMN concentration and a variable NADH concentration in the presence of AMP (a dead-end inhibitor), a Lineweaver−Burk plot demonstrated competitive inhibition by AMP (Figure 4A) with a K_i of 11.1 mM. When the activity in the presence of AMP was determined at a fixed NADH concentration and a variable FMN concentration, a similar plot revealed noncompetitive inhibition (Figure 4B). The activity of FRD$_{Aa}$ was also measured in the presence of

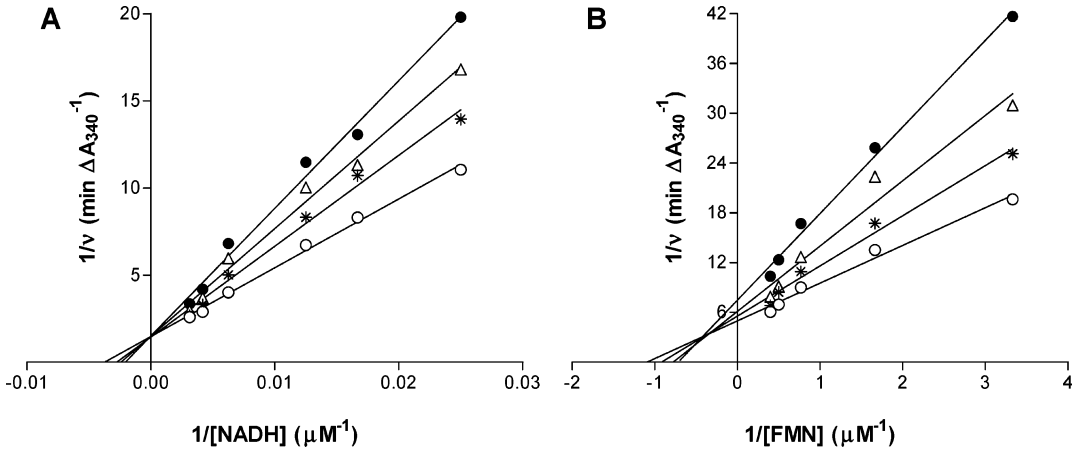

FIGURE 4: Dead-end inhibition of FRD_{Aa} with AMP: (A) ν as a function of NADH concentration using 1.3 μM FMN without (○) or with 3.2 (∗), 7 (△), and 10 (●) mM AMP; (B) ν as a function of FMN concentration using 60 μM NADH without (○) or with 3.2 (∗), 7 (△), and 10 (●) mM AMP.

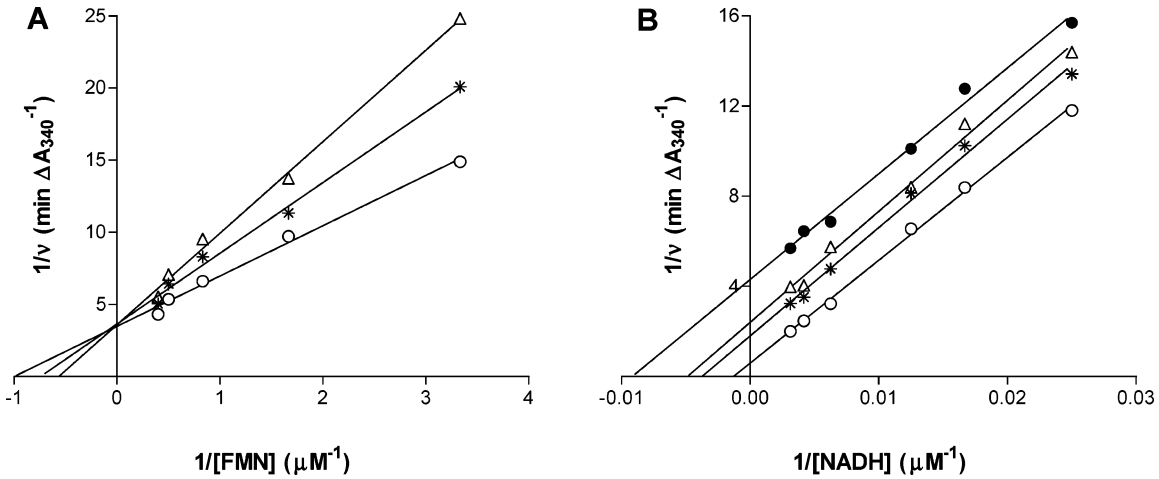

FIGURE 5: Inhibition of FRD_{Aa} with lumichrome: (A) ν as a function of FMN concentration using 80 μM NADH without (○) or with 100 (∗) and 200 (△) μM lumichrome; (B) ν as a function of NADH concentration using 1.3 μM FMN without (○) or with 50 (∗), 100 (△), and 200 (●) μM lumichrome.

the flavin analogue lumichrome, which has no substrate activity. At a fixed NADH concentration and variable FMN concentrations, a competitive inhibition pattern was found for lumichrome (Figure 5A) with a K_i of 0.25 mM. The activities at a fixed FMN concentration and variable NADH concentrations show uncompetitive inhibition by lumichrome (Figure 5B). These data support that FRD utilizes an ordered sequential mechanism with NADH as the first substrate and FMN as the second (*34*).

The order of product release was also determined by patterns of inhibition by the product NAD^+ (*35*). When the concentration of NADH was varied at a fixed concentration of FMN, competitive inhibition occurred (Figure 6A) with a K_i of 4.9 mM for NAD^+. When FMN was varied at a fixed NADH concentration, noncompetitive inhibition was indicated (Figure 6B). These kinetic patterns indicate that the first product to be released is $FMNH_2$ and that the second is NAD^+. The overall kinetic mechanism is summarized in Scheme 1, in which E is the FRD apoenzyme, F and FH are, respectively, the oxidized and reduced forms of the cofactor, N and NH are, respectively, NAD^+ and NADH, and f and fH are, respectively, the oxidized flavin substrate and the reduced flavin product.

CD Spectra. The CD spectrum of the native FRD_{Aa} (containing one FMN per dimeric enzyme) and that with 92% of the bound FMN removed were determined. The two samples showed essentially identical CD spectra (data not shown).

Scheme 1

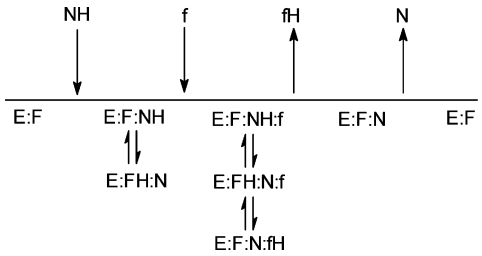

Anaerobic Reduction of Native FRD_{Aa} by NADH. Upon mixing 53 μM native FRD_{Aa} (containing 16 μM bound FMN) with 1.1 mM NADH under anaerobic conditions, the bound FMN was immediately and fully reduced within the manual mixing time (Figure 7, line 1). The spectrum of the reduced enzyme remained unchanged over a period of 60 min (spectra not shown). When the reaction cuvette was opened to the air, the spectrum gradually returned to the fully oxidized form (Figure 7, lines 2−4) over a period of about 32 min when all the excess NADH was oxidized. Very little, and probably insignificant, absorption was detected at >520 nm for all samples.

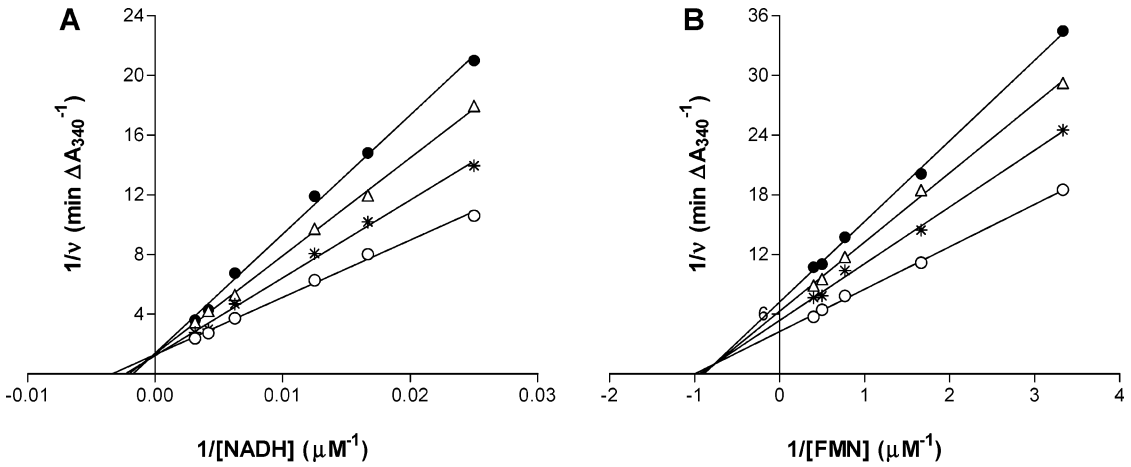

FIGURE 6: Inhibition of FRD_{Aa} with NAD^+: (A) ν as a function of NADH concentration using 1.3 μM FMN without (○) or with 1.2 (∗), 3.2 (△), and 8 (●) mM NAD^+; (B) ν as a function of FMN concentration using 60 μM NADH without (○) or with 1.2 (∗), 3.2 (△), and 5 (●) mM NAD^+.

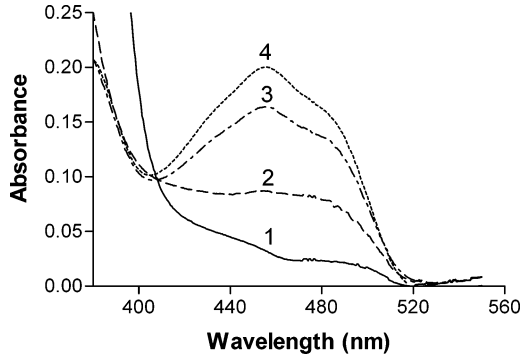

FIGURE 7: Anaerobic reduction and reoxidation of FRD_{Aa}-bound FMN. FRD_{Aa} was 53 μM with 16 μM bound FMN. FMN was reduced anaerobically by the addition of a final concentration of 1.1 mM NADH. Spectrum 1 was obtained immediately following reduction, spectra 2 and 3 were the transient spectra during partial reoxidation, and spectrum 4 was obtained after complete reoxidation.

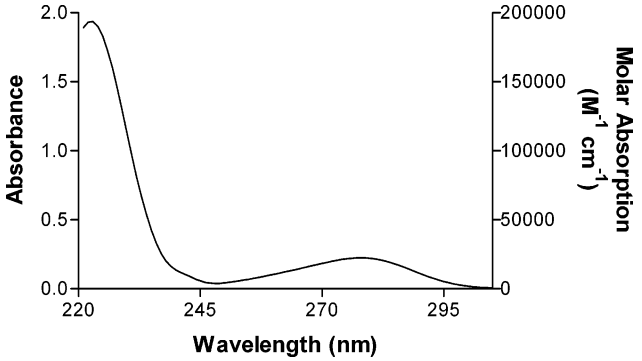

FIGURE 8: Globally fitted extinction profile of FRD_{Aa} with bound FMN.

Subunit Interaction of FRD_{Aa}. To establish the associative properties of FRD_{Aa} with bound FMN, equilibrium sedimentation experiments were conducted. To ensure a good signal from both the monomer and dimer species, a large concentration range of protein was used for generating the experimental data. This was accomplished by varying the loading concentration and the wavelength of the measurement, which exploited the various absorption properties of FRD_{Aa}. Rayleigh interference data were also included to produce a comprehensive global fit. Globally fitting data observed under multiple conditions (such as multiple rotor speeds and multiple loading concentrations) is ideal since it is possible to enhance the confidence in each fitted parameter value (*36*). In such a fit, parameters such as monomer molecular mass and association constants are considered global parameters and forced to be the same for all included data sets. To compensate for the different absorption properties at different wavelengths, we measured wavelength scans between 220 and 350 nm using 1 nm intervals in triplicate with 20 repetitions for each datum point. The wavelength scans were globally fitted to a sum of Gaussian terms, whose width, amplitude, and offset were allowed to float but were considered global for all scans. Individual concentrations were adjusted by floating the amplitude of the sum for each scan. The resulting molar absorption profile (Figure 8) was normalized by using an estimated molar absorption coefficient at 280 nm from the sequence of the denatured protein determined by the method of Gill and von Hippel. The refractive index properties of FRD_{Aa} were estimated to be 3.28 (fringes/mg)/mL and used to correct the interference data in the global fit.

Fits of the experimental data to a monomer−dimer model provided consistently random residuals over all measured concentrations, wavelengths, speeds, and optical systems (Figure 9) when interference data up to 2 fringes in concentration were included. Measurements of higher fringes also indicated the presence of higher ordered species, but it was impossible to fit the data to a global self-associating model (such as a monomer−dimer−tetramer or monomer−dimer−trimer−tetramer model) and retain random residuals (data not shown). This indicates a minor contribution by some irreversibly aggregated species. By limiting the fringes to a value of 2, this contribution could be effectively excluded from the fit. The monomer−dimer fit resulted in a monomer molecular mass of 35.34 kDa (+0.60 kDa/−0.49 kDa), which is in excellent agreement with the theoretical monomer molecular mass derived from the peptide sequence. The monomer−dimer K_d was determined to be 2.7 ± 0.7 μM, which indicates tight dimerization. The relative distribution of monomer and dimer versus total concentration is shown in Figure 10. This plot is based on the equilibrium constant determined in the global fit of 25 equilibrium scans.

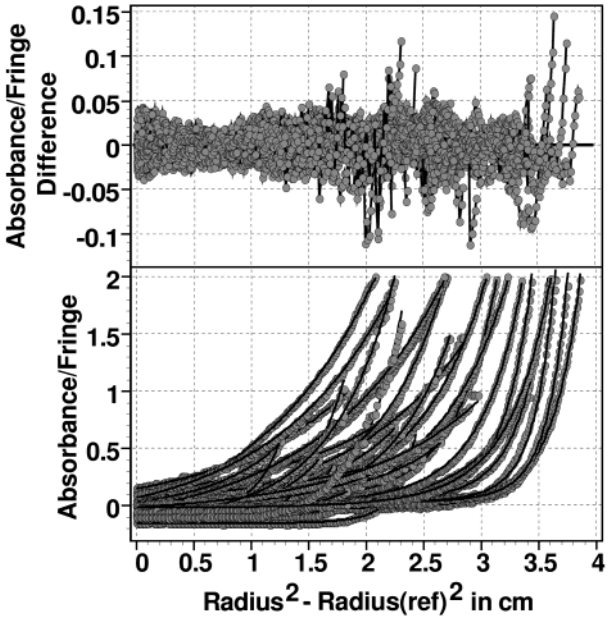

FIGURE 9: Experimental sedimentation equilibrium scans of FRD_{Aa} with bound FMN at multiple loading concentrations, speeds, and wavelengths using both interference and absorption optical data. Absorption data were used up to 0.9 absorbance unit, and interference data were used up to 2.0 fringes. Wavelengths, loading concentrations, and speeds were configured as described in the Experimental Procedures. All scans were simultaneously fitted to a global monomer−dimer model. Residuals of the fit are shown above. Fitted curves are shown as lines overlayed on top of the experimental data, which are displayed as circles. In addition to the absorbance at 230 and 280 nm, the ordinate also indicates the number of fringes for the interference measurements on the same scale.

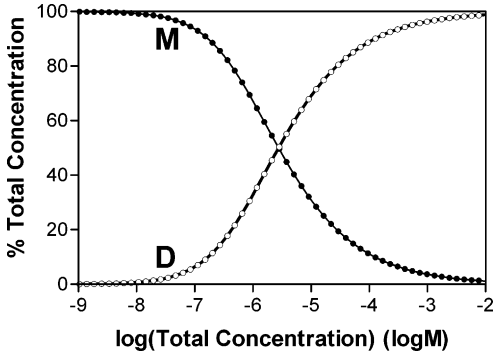

FIGURE 10: Distribution of the relative monomer and dimer concentration versus the total molar concentration. Open circles indicate the relative concentration of the dimer, and filled circles represent the relative concentration of the monomer. The distributions are based on the equilibrium constant determined in the global fit of 25 equilibrium scans. As the concentration increases above the K_d level, the dimer becomes the predominant species.

DISCUSSION

The growing recognition of their physiological functions and their structural and mechanistic variety makes flavin reductases challenging and intriguing systems to analyze. Among known flavin reductases, most lacking in understanding are genuine FRD enzymes, either flavoenzyme class I or nonflavoenzyme class II. The FMN-containing flavin reductase NmoB or NtaB from *A. aminovorans* was reported to be an FRD (*18*) and, hence, was chosen for detailed characterization in this work.

First, the general properties of FRD_{Aa} were examined with respect to purification yields, thermal stability, pI value, molar absorption coefficient, effect of phosphate buffer strength on activity, and the pH−activity profile. The pH−activity profile is interesting in that it is bimodal, with the primary pH optimum at 8.5 and a minor peak at pH 5.2 (Figure 1). This FRD_{Aa} was originally purified as one of two enzymes within a nitrilotriacetate monooxygenase complex; the other component is a monofunctional nitrilotriacetate monooxygenase that can hydroxylate the nitrilotriacetate but cannot reduce flavin (*18*). The two-component monooxygenase complex shows a maximal activity at pH 8.5 (*18*), identical to that for the primary activity peak of the isolated FRD_{Aa}. Hence, FRD_{Aa} is likely to be important to the regulation of the two-component nitrilotriacetate monooxygenase complex with respect to the optimal pH for the coupled activity.

One unusual aspect of FRD_{Aa} reported earlier is the amount of bound FMN in the purified enzyme. Uetz et al. (*18*) found that FMN fell off from the enzyme during purification, ending up with 0.1−0.4 mol of bound FMN per FRD_{Aa} dimer. Moreover, only one bound FMN per FRD_{Aa} dimer was obtained when the enzyme was saturated with exogenously added FMN (*18*). Since native FRD_{Aa} is an identical dimer, a maximal one bound FMN per dimer would be difficult to rationalize structurally or catalytically. We found that the ratio of FMN bound to FRD_{Aa} was also somewhat variable following each purification preparation, but there was typically one FMN bound per dimer. However, our results differ from those of Uetz et al. in that one FMN per monomer was found under saturating FMN conditions as shown by equilibrium ultrafiltration and by fluorometric titration. The latter study also revealed a K_d of 0.6 μM for the FMN cofactor binding. Although with a weaker binding affinity, native FRD_{Aa} can also bind riboflavin to a total content of one bound flavin per monomeric enzyme.

The kinetic mechanism of FRD_{Aa} was determined by steady-state kinetic analysis of initial rates at various concentrations of the two substrates and with respect to patterns of inhibition by dead-end inhibitors and the NAD^+ product. Double reciprocal plots of initial rates versus varying concentrations of FMN and several fixed levels of NADH (Figure 3A) and varying levels of NADH at several constant amounts of FMN (Figure 3B) both reveal a pattern of converging lines. Therefore, a sequential Bi Bi mechanism is indicated. Values of $K_{m,NADH} = 0.35$ mM and $K_{m,FMN} = 1.3$ μM are identical to those previously determined (*18*). The maximal specific activity (8.4 ± 1.3 (μmol/min)/mg) varied somewhat. It probably has to do with the very high K_m for NADH, which makes it difficult to carry out spectrophotometric assays using NADH concentrations close to or above its K_m.

FRD_{Aa} also utilized riboflavin and FAD as a substrate. In comparison with FMN, FAD exhibited similar K_m and V_{max} values whereas riboflavin had higher values in both. As dictated by the sequential mechanism, both the NADH and flavin substrates must be bound by the FRD_{Aa} active site to effect catalysis. The finding that FAD was similar to FMN in K_m value suggests that there is no significant overlap of the binding site for the AMP moiety of FAD with that for NADH. This is quite different from the *E. coli* Fre for which the FAD site overlaps with that of NADH or NADPH (*3*).

Patterns of inhibition by AMP (Figure 4) and lumichrome (Figure 5) were investigated to identify further the sequence of NADH and FMN binding. Results of these studies are all consistent with an ordered sequential mechanism in which NADH binds prior to FMN. Furthermore, patterns of inhibition by the NAD^+ product (Figure 6) also indicate that $FMNH_2$ was released as a product prior to NAD^+.

One highly surprising finding is that FRD_{Aa}, unlike the class I *V. harveyi* FRP and *V. fischeri* FRG, exhibited a sequential rather than the expected ping-pong mechanism. Following the sequential mechanism, both NADH and FMN substrates are bound to the FRD_{Aa} active site for the exchange of reducing equivalents. Hence, the presence of a bound flavin cofactor is not obligatory for catalysis. Three possibilities for the functional role of the FMN initially bound to and coisolated with native FRD_{Aa} are hypothesized. (1) The bound FMN does not participate in catalysis. Instead, it serves a structural purpose, maintaining FRD_{Aa} in a particular active conformation. (2) The bound FMN is a substrate. (3) It is a genuine but unusual type of cofactor. NADH and substrate FMN form a quaternary complex with FRD_{Aa} and cofactor FMN, where the cofactor FMN directly shuttles reducing equivalents between NADH and substrate FMN (Scheme 1).

To examine the first possibility, the CD spectra of the native FRD_{Aa} and a sample containing only 8% of the bound FMN were compared and found to be identical (data not shown). By this criterion, the binding of FMN did not result in any detectable conformational change of the FRD_{Aa} protein. A more telling test is the anaerobic reduction of the native FRD_{Aa}-bound FMN by NADH (Figure 7). Clearly the bound FMN is not redox inert. On the basis of these two tests, the first possibility can be ruled out. The second possibility that the bound FMN is a substrate rather than cofactor is contrary to the kinetic mechanism determined in this work. Patterns of inhibition by the dead-end inhibitors AMP (Figure 4) and lumichrome (Figure 5) clearly indicated that the sequence of substrate binding is NADH before, not after, flavin. If one argues that the prebound FMN is a substrate, which was shown to be redox active upon subsequent addition of NADH (Figure 7), then the sequence of substrate binding would be FMN before NADH. The third possibility that the bound FMN is an unusual cofactor is depicted in Scheme 1. This scheme is, at the present, consistent with all available experimental results. In the absence of NADH, FRD_{Aa} can bind a maximum of one flavin cofactor per monomeric enzyme. Moreover, the bound FMN is redox active. By considering the prebound FMN as a cofactor, Scheme 1 can account for the redox activity of this bound FMN, the inability of apoFRD_{Aa} to bind NADH (tested up to 90 and 300 μM, respectively), and the ordered sequential kinetic mechanism involving the binding of NADH to holoenzyme prior to the FMN substrate. A number of experimental tests will be under way to further examine the validity of this scheme and to determine some of the kinetic constants. Even in the absence of additional new information, it is clear that FRD_{Aa} is a rather unusual flavin reductase containing a bound FMN.

A recent report (*37*) on the *Streptomyces coelicolor* flavin reductase ActVB, which is involved in the last step of the biosynthesis of the antibiotic actinorhodin, provides a very interesting case for comparison with FRD_{Aa}. There are a number of parallels between these two reductases. While the FRD_{Aa} monomer is about twice the size of ActVB (34.5 kDa versus 18 kDa), both can exist as a homodimer and share significant sequence similarity and identity over approximately the first 170 residues. The isolated ActVB contains varying amounts of bound FMN, and belongs to the FRD type highly specific for NADH. Moreover, ActVB follows an ordered sequential mechanism with NADH binding prior to that by flavin. However, FRD_{Aa} differs from ActVB in that the former releases $FMNH_2$ first whereas ActVB releases NAD^+ as the first product. The charge-transfer complex of reduced FMN and NAD^+ observed with ActVB was not detected in FRD_{Aa}. Last but not least, Filisetti et al. (*37*) concluded that the bound FMN in ActVB is a substrate rather than a cofactor. However, such a conclusion is inconsistent with their finding that NADH can reduce the prebound FMN. It is important to note that other enzymes in the FRD family, VlmR (FRP class I) from *Streptomyces viridifaciens* (*38*) and SnaC (FRD class I) from *Streptomyces pristinaespiralis* (*39*), have bound flavin as well. However, the functional roles of the bound flavin in these two cases have not been characterized.

Both the *V. harveyi* FRP and the *V. fischeri* FRP/FRase I undergo monomer−dimer equilibrium with K_d values of 1.8 μM (*7*) and 13.4 μM (*11*), respectively. More importantly, such a subunit monomer−dimer equilibrium is physiologically important in the case of *V. harveyi* FRP. Only the monomeric FRP forms a complex with luciferase, and FRP is essentially all trapped in a monomer form in a functional complex with luciferase in vivo (*22*, *40*). Therefore, it is important to also characterize the quaternary structure of FRD_{Aa}. We found that FRD_{Aa} exhibited a monomer−dimer equilibrium as well with a K_d of 2.7 μM. It was determined that the two-component NTA monooxygenase complex was 7% of the total cellular protein from *C. heintzii* (*18*). A cell volume of 1 μm^3 was assumed to determine an in vivo concentration of NTA monooxygenase of 5 mg/mL. It was also assumed that FRD_{Aa} and the NTA monooxygenase exist in a 1:1 molar ratio within the two-component complex (*19*). As an extension of this, the cellular content of FRD_{Aa} can be estimated to be about 72 μM on the basis of monomer molecular weight. In the absence of the NTA monooxygenase, FRD_{Aa} would exist primarily as a dimer in vivo. Quantitative effects of the NTA monooxygenase on the quaternary structure of FRD_{Aa} remain to be determined.

For canonical flavoenzymes, the flavin cofactor remains bound to the enzyme and shuttles between oxidized and reduced forms during the catalytic cycle. The flavin cofactor is regenerated to the original redox form upon completion of each turnover. Ever since the discovery of flavin cofactors in the 1930s, numerous and diverse types of flavoenzymes have been shown to share common features as stated above. In contrast, flavin reductases produce and subsequently release dihydroflavin as a product that is essential as a substrate for a number of reduced flavin-acceptor enzymes or as a critical metabolite for some biological functions (*1*). While some flavin reductases are flavoenzymes containing a bound flavin cofactor, others are not. One interesting feature gradually emerging from studies on flavin reductases is that, for those reductases that contain bound flavin, the functional role of the bound flavin is often unconventional. Individual *V. harveyi* FRP and *V. fischeri* FRG are, by all conventional

criteria, genuine flavoenzymes. Both undergo a ping-pong mechanism involving the bound FMN as a redox cofactor (*41*, *42*). However, when they are coupled with their respective luciferase, the bound FMN actually behaves as a substrate in that it is directly transferred to luciferase after its reduction to leave the reductase in an apoenzyme form and the kinetic mechanism changes from the ping-pong type to sequential (*41*, *42*). In the present case of FRD_{Aa}, the bound FMN may still be a cofactor, but its catalytic role is rather unusual to allow a sequential mechanism. As for ActVB, the bound FMN was proposed to be a substrate (*37*) although, as stated above, not all experimental results are consistent with such a role. As the list grows and more enzymes are studied, the surprises that flavin reductases provide will likely grow as well.

ACKNOWLEDGMENT

We thank Dr. Luying Xun of Washington State University for his generous gift of the pTF2 plasmid. We thank Dr. Glen Legge for allowing us to use the circular spectropolarimeter. We also thank Samer Kabbara for technical assistance.

REFERENCES

1. Tu, S.-C. (2001) Reduced flavin: Donor and acceptor enzymes and mechanisms of channeling, *Antioxid. Redox Signaling 3*, 881−897.
2. Fieschi, F., Nivière, V., Frier, C., Décout, J.-L., and Fontecave, M. (1995) The mechanism and substrate specificity of the NADPH:flavin oxidoreductase from *Escherichia coli*, *J. Biol. Chem. 270*, 30392−30400.
3. Louie, T. M., Yang, H., Karnchanaphanurach, P., Xie, X. S., and Xun, L. (2002) FAD is a preferred substrate and an inhibitor of *Escherichia coli* general NAD(P)H:flavin oxidoreductase, *J. Biol. Chem. 277*, 39450−39455.
4. Gerlo, E., and Charlier, J. (1975) Identification of NADH-specific and NADPH-specific FMN reductases in *Beneckea harveyi*, *Eur. J. Biochem. 57*, 461−467.
5. Jablonski, E., and DeLuca, M. (1978) Studies of the control of luminescence in *Beneckea harveyi*: properties of the NADH and NADPH:FMN oxidoreductases, *Biochemistry 17*, 672−678.
6. Lei, B., Liu, M., Huang, S., and Tu, S.-C. (1994) *Vibrio harveyi* NADPH-flavin oxidoreductase: cloning, sequencing and overexpression of the gene and purification and characterization of the cloned enzyme, *J. Bacteriol. 176*, 3552−3558.
7. Liu, M., Lei, B., Ding, Q., Lee, J. C., and Tu, S.-C. (1997) *Vibrio harveyi* NADPH:FMN oxidoreductase: preparation and characterization of the apoenzyme and monomer−dimer equilibrium, *Arch. Biochem. Biophys. 337*, 89−95.
8. Tanner, J. J., Lei, B., Tu, S.-C., and Krause, K. L. (1996) Flavin reductase P: structure of a dimeric enzyme that reduces flavin, *Biochemistry 35*, 13531−13539.
9. Inouye, S. (1994) NAD(P)H-flavin oxidoreductase from the bioluminescent bacterium, *Vibrio fischeri* ATCC 7744, is a flavoprotein, *FEBS Lett. 347*, 163−168.
10. Zenno, S., Saigo, K., Kanoh, H., and Inouye, S. (1994) Identification of the gene encoding the major NAD(P)H-flavin oxidoreductase of the bioluminescent bacterium *Vibrio fischeri* ATCC 7744, *J. Bacteriol. 176*, 3536−3543.
11. Tang, C. K., Jeffers, C. E., Nichols, J. C., and Tu, S. C. (2001) Flavin specificity and subunit interaction of *Vibrio fischeri* general NAD(P)H-flavin oxidoreductase FRG/FRase I, *Arch. Biochem. Biophys. 392*, 110−116.
12. Koike, H., Sasaki, H., Kobori, T., Zenno, S., Saigo, K., Murphy, M. E., Adman, E. T., and Tanokura, M. (1998) 1.8 Å crystal structure of the major NAD(P)H:FMN oxidoreductase of a bioluminescent bacterium, *Vibrio fischeri*: overall structure, cofactor and substrate-analog binding, and comparison with related flavoproteins, *J. Mol. Biol. 280*, 259−273.
13. Spyrou, G., Haggard-Ljungquist, E., Krook, M., Jornvall, H., Nilsson, E., and Reichard, P. (1991) Characterization of the flavin reductase gene (*fre*) of *Escherichia coli* and construction of a plasmid for overproduction of the enzyme, *J. Bacteriol. 173*, 3673−3679.
14. Nivière, V., Fieschi, F., Décout, J.-L., and Fontecave, M. (1999) The NAD(P)H:flavin oxidoreductase from *Escherichia coli*. Evidence for a new mode of binding for reduced pyridine nucleotides, *J. Biol. Chem. 274*, 18252−18260.
15. Nivière, V., Fieschi, F., Décout, J.-L., and Fontecave, M. (1996) Is the NAD(P)H:flavin oxidoreductase from *Escherichia coli* a member of the ferredoxin-$NADP^+$ reductase family? Evidence for the catalytic role of serine 49 residue, *J. Biol. Chem. 271*, 16656−16661.
16. Nivière, V., Vanoni, M. A., Zanetti, G., and Fontecave, M. (1998) Reaction of NAD(P)H:flavin oxidoreductase from *Escherichia coli* with NADPH and riboflavin: Identification of intermediates, *Biochemistry 37*, 11879−11887.
17. Ingelman, M., Ramaswamy, S., Nivière, V., Fontecave, M., and Eklund, H. (1999) Crystal structure of NAD(P)H:flavin oxidoreductase from *Escherichia coli*, *Biochemistry 38*, 7040−7049.
18. Uetz, T., Schneider, R., Snozzi, M., and Egli, T. (1992) Purification and characterization of a two-component monooxygenase that hydroxylates nitrilotriacetate from "*Chelatobacter*" strain ATCC 29600, *J. Bacteriol. 174*, 1179−1188.
19. Knobel, H. R., Egli, T., and van der Meer, J. R. (1996) Cloning and characterization of the genes encoding nitrilotriacetate monooxygenase of *Chelatobacter heintzii* ATCC 29600, *J. Bacteriol. 178*, 6123−6132.
20. Xu, Y., Mortimer, M. W., Fisher, T. S., Kahn, M. L., Brockman, F. J., and Xun, L. (1997) Cloning, sequencing, and analysis of a gene cluster from *Chelatobacter heintzii* ATCC 29600 encoding nitrilotriacetate monooxygenase and NADH:flavin mononucleotide oxidoreductase, *J. Bacteriol. 179*, 1112−1116.
21. Bucheli-Witschel, M., and Egli, T. (2001) Environmental fate and microbial degradation of aminopolycarboxylic acids, *FEMS Microbiol. Rev. 25*, 69−106.
22. Jeffers, C. E., Nichols, J. C., and Tu, S.-C. (2003) Complex formation between *Vibrio harveyi* luciferase and monomeric NADPH:FMN oxidoreductase, *Biochemistry 42*, 529−534.
23. Russell, T. R., and Tu, S.-C. (2003) The Kinetic Mechanism of NADH:Flavin Oxidoreductase from *Chelatobacter heintzii* ATCC 29600, 5th European Symposium of the Protein Society, Abstract 548.
24. Ausubel, M. F. (1993) *Current Protocols in Molecular Biology*, John Wiley & Sons: New York.
25. Gill, S. C., and von Hippel, P. H. (1989) Calculation of protein extinction coefficients from amino acid sequence data, *Anal. Biochem. 182*, 319−326.
26. Kendrew, S. G., Harding, S. E., Hopwood, D. A., and Marsh, E. N. (1995) Identification of a flavin:NADH oxidoreductase involved in the biosynthesis of actinorhodin. Purification and characterization of the recombinant enzyme, *J. Biol. Chem. 270*, 17339−17343.
27. Tu, S.-C., and McCormick, D. B. (1974) Conformation of porcine D-amino acid oxidase as studied by protein fluorescence and optical rotatory dispersion, *Biochemistry 13*, 893−899.
28. Laue, T. M., Shah, B. D., Ridgeway, T. M., and Pelletier, S. L. (1992) Computer-Aided Interpretation of Analytical Sedimentation Data For Proteins, in *Analytical Ultracentrifugation in Biochemistry and Polymer Science* (Harding, S. E., Rowe, A. J., and Horton, J. C., Eds.) pp 106−107, Royal Society of Chemistry, Cambridge, England.
29. Durchschlag, H. (1986) Specific Volumes of Biological Macromolecules and Some Other Molecules of Biological Interest, in *Thermodynamic Data for Biochemistry and Biotechnology* (Hinz, H.-J., Ed.) pp 45−128, Springer-Verlag, New York.
30. Bradford, M. M. (1976) A rapid and sensitive method for the quantitation of microgram quantities of protein utilizing the principle of protein-dye binding, *Anal. Biochem. 72*, 248−254.
31. Lowry, O. H., Rosebrough, N. J., Farr, A. L., and Randall, R. J. (1951) *J. Biol. Chem. 193*, 265−275.
32. Fromm, H. J. (1979) Summary of kinetic reaction mechanisms, *Methods Enzymol. 63*, 42−53.
33. Cleland, W. W. (1963) The Kinetics of Enzyme-Catalyzed Reactions with Two or More Substrates or Products, *Biochim. Biophys. Acta* 67, 104−137.
34. Fromm, J. H. (1979) Use of competitive inhibitors to study substrate binding order, *Methods Enzymol. 63*, 467−486.

35. Rudolph, F. B. (1979) Product inhibition and abortive complex formation, *Methods Enzymol. 63*, 411−436.
36. Johnson, M. L., Correia, J. J., Yphantis, D. A., and Halvorson, H. R. (1981) Analysis of data from the analytical ultracentrifuge by nonlinear least- squares techniques, *Biophys. J. 36*, 575−588.
37. Filisetti, L., Fontecave, M., and Niviere, V. (2003) Mechanism and substrate specificity of the flavin reductase ActVB from *Streptomyces coelicolor*, *J. Biol. Chem. 278*, 296−303.
38. Parry, R. J., and Li, W. (1997) An NADPH:FAD oxidoreductase from the valanimycin producer, *Streptomyces viridifaciens*. Cloning, analysis, and overexpression, *J. Biol. Chem. 272*, 23303−23311.
39. Blanc, V., Lagneaux, D., Didier, P., Gil, P., Lacroix, P., and Crouzet, J. (1995) Cloning and analysis of structural genes from *Streptomyces pristinaespiralis* encoding enzymes involved in the conversion of pristinamycin IIB to pristinamycin IIA (PIIA): PIIA synthase and NADH:riboflavin 5′-phosphate oxidoreductase, *J. Bacteriol. 177*, 5206−5214.
40. Low, J. C., and Tu, S.-C. (2003) Energy transfer evidence for *in vitro* and *in vivo* complexes of *Vibrio harveyi* flavin reductase P and luciferase, *Photochem. Photobiol. 77*, 446−452.
41. Lei, B., and Tu, S.-C. (1998) Mechanism of reduced flavin transfer from *Vibrio harveyi* NADPH−FMN oxidoreductase to luciferase, *Biochemistry 37*, 14623−14629.
42. Jeffers, C. E., and Tu, S.-C. (2001) Differential transfers of reduced flavin cofactor and product by bacterial flavin reductase to luciferase, *Biochemistry 40*, 1749−1754.

BI035578A